# Development of an equation of state for electrolyte solutions by combining the statistical associating fluid theory and the mean spherical approximation for the nonprimitive model

Honggang Zhao, M. Carolina dos Ramos, and Clare McCabe[a)]
*Department of Chemical Engineering, Vanderbilt University, Nashville, Tennessee 37235*

(Received 19 February 2007; accepted 30 March 2007; published online 22 June 2007)

A statistical associating fluid theory to model electrolyte fluids that explicitly accounts for solvent molecules by modeling water as a dipolar square-well associating fluid is presented. Specifically the statistical associating fluid theory for potentials of variable range (SAFT-VR) is combined with integral equation theory and the generalized mean spherical approximation using the nonprimitive model to describe the long-range ion-ion, ion-dipole, and dipole-dipole interactions. Isothermal-isobaric ensemble Monte Carlo simulations have been performed in order to test the new theoretical approach. In particular, simulations are performed for different ion concentrations and different ratios of the cation, anion, and solvent segment diameters. Predictions for the thermodynamic properties from the new equation of state are compared with the computer simulation data. Additionally, results from a combination of the SAFT-VR approach with Debye-Hückel theory and the primitive model are also presented and compared to those obtained with the nonprimitive model to illustrate the advantages of the new statistical associating fluid theory for potentials of variable range plus dipole and electrolytes (SAFT−VR+DE) approach. The results show that the proposed equation of state provides a good description of the *PVT* properties of electrolyte fluids with different sizes of ions and solvent. © *2007 American Institute of Physics*. [DOI: 10.1063/1.2733673]

## I. INTRODUCTION

Electrolyte solutions, and in particular, aqueous electrolyte solutions, are central to chemical, biological, and environmental processes. The thermodynamic properties of electrolyte solutions are therefore crucial to the design and operation of processes such as protein separations, in addition to applications in the more traditional chemical and petroleum industries. The importance of understanding the thermodynamics of electrolyte solutions is reflected by the significant body of work devoted to developing theoretical tools to predict their thermodynamic and physical properties.

One of the key barriers to the development of predictive approaches for electrolyte solutions is the complexity of the interactions and the need to describe the long-range charge-charge and charge-polar interactions. Several theoretical models have been developed to specifically deal with these interactions in electrolyte solutions.[1] In particular, the Debye-Hückel theory was the first theory for electrolyte solutions and considers the ions to be point charges, and so does not include the effect of the volume of the ions and treats the solvent as a dielectric continuum. The Debye-Hückel approach provides a good description of low concentration electrolyte solutions and has been used to develop many semiempirical equations of state (EOSs) such as the Pitzer[2] equations and the electrolyte nonrandom two-liquid[3] model.

Perturbation theory was first applied by Stell and Lebowitz[4] to model electrolyte solutions using the hard sphere as a reference state and Debye-Hückel theory to deduce the perturbation term of the Helmholtz free energy for the ion-ion interaction. Henderson later[5] proposed a restricted perturbation theory in which the ion-ion interaction is treated as a perturbation term. Both approaches model the solvent as a continuous medium and hence are McMillan-Mayer (MM) level of models [as opposed to Born-Oppenheimer (BO) models that explicitly include the solvent].[6] MM models, in which the ions are hard spheres, are referred to as primitive models.[7] Subsequently, Henderson *et al.*[8] extended their approach to ion-dipole mixtures. Chan[9] later applied this model to simple chloride solutions and found that the nonprimitive model, which explicitly models the solvent as dipolar molecules, did not give better results than the primitive model, despite the more realistic nature of the model. The apparent failure was attributed to inaccurate predictions of the reference hard-sphere fluid properties. In an alternative approach, Jin and Donohue[10] combined the perturbed-anisotropic-chain theory[11] for short-range interactions between molecules with Henderson's primitive model for the long-range Coulombic interactions and studied a range of single and multiple electrolyte solutions.

As an alternative to perturbation theory, a number of equations for electrolyte solutions have been proposed based on integral equation theory. Within integral equation theory, two important approximations, the hypernetted chain (HNC) and the mean spherical approximation (MSA), have been

[a)]Author to whom correspondence should be addressed. Electronic mail: c.mccabe@vanderbilt.edu

 

used to solve the Ornstein-Zernike equation for electrolyte fluids. However, while the HNC[12] approximation is the more accurate, it is mathematically complex and does not provide analytical solutions. For example, an important HNC theory is the reference interaction site model, developed by Chandler and Andersen[13] and Rossky and co-workers,[14] which takes into account the molecular shape of the ions and solvent; however, it yields a trivial dielectric constant for the solvent in BO models and the solution is not analytic, requiring numerical methods. In contrast, the MSA allows for analytical solutions to be developed for a wide range of model fluids.[15] Independently, Waisman and Lebowitz[16] and Blum[17] obtained analytical expressions for the thermodynamic properties of the restricted and unrestricted primitive MSA models, respectively (restricted refers to primitive models in which the ions are hard spheres of equal diameter and opposite signs). The primitive MSA (PMSA) accounts for the effect of the volume of the ions explicitly; when the diameters of the ions vanish the MSA expression reduces to the Debye-Hückel equation. The PMSA model has been applied to develop equations of state for electrolyte fluids by several authors.[18] For example, Ball *et al.*[19] established an EOS for electrolyte solutions that uses the PMSA to describe the long-range interactions, and Lu *et al.*[20] have used the PMSA to calculate the activity coefficients of single and mixed aqueous electrolyte solutions using ionic-strength-dependent effective diameters for the cation.

To explicitly account for the effect of the solvent, Blum[21] and Adelman and Deutch[22] developed analytic solutions for the nonprimitive MSA (NPMSA) model, yielding expressions for the thermodynamic properties of a mixture of equal sized ions and dipolar hard spheres. Blum and Wei[23] later extended the solutions to the system of arbitrary sizes of charged and dipolar hard spheres. The solution of the NPMSA includes three types of interaction: ion-ion, ion-dipole, and dipole-dipole interactions. Hoye and Stell[24] have used the approach of Blum and Wei to yield explicit forms for the ion-ion, ion-dipole, and dipole-dipole pair distribution functions. Li *et al.*[25] subsequently tested the NPMSA against Monte Carlo simulation data and found that while it provides a good description of the ion-ion contribution to the internal energy, the ion-dipole contribution is underestimated. For a comprehensive review of theories developed for aqueous electrolyte fluids, the reader is directed to the excellent reviews of Loehe and Donohue[26] and Anderko *et al.*[27]

In this work we propose a new equation of state for electrolyte fluids that combines the analytical results of the MSA with an accurate model for the short-range dispersion and association interactions, which also play an important role in determining the thermodynamic properties of electrolyte systems. Through a combination of integral equation theory and perturbation theory, within the framework of the statistical associating fluid theory (SAFT), we can develop a statistical mechanics based model that accurately captures the key molecular level interactions. The statistical associating fluid theory was proposed by Chapman *et al.*[28] based on Wertheim's thermodynamic perturbation theory for association,[29] and explicitly takes into account the effect of nonsphericity and association interactions. In recent years SAFT has proven to be a powerful equation of state for modeling associating and nonassociating chain fluids and their mixtures (see, for example, the numerous applications highlighted in a recent review of the SAFT equation[30]). In the SAFT approach, the free energy is written as the sum of four separate contributions:

$$\frac{A}{Nk_BT} = \frac{A^{\text{ideal}}}{Nk_BT} + \frac{A^{\text{mono}}}{Nk_BT} + \frac{A^{\text{chain}}}{Nk_BT} + \frac{A^{\text{assoc}}}{Nk_BT}, \tag{1}$$

where $N$ is the number of molecules, $k_B$ Boltzmann's constant, and $T$ the temperature. $A^{\text{ideal}}$ is the ideal free energy, $A^{\text{mono}}$ the contribution to the free energy due to the monomer segments, $A^{\text{chain}}$ the contribution due to the formation of bonds between monomer segments, and $A^{\text{assoc}}$ the contribution due to association. Hence, a SAFT fluid is a collection of monomers that can form covalent bonds; the monomers interact via repulsive and attractive (dispersion) forces and, in some cases, association interactions. Within the SAFT framework, many extensions of the original equations have been proposed. These essentially correspond to different choices for the monomer fluid, and different theoretical approaches to the calculation of the monomer free energy and structure.[31] In this work we focus on SAFT-VR, which describes chain molecules formed from hard-core monomers with attractive potentials of variable range (SAFT-VR),[32,33] typically a square well. The SAFT-VR equation has been successfully used to describe the phase equilibria of a wide range of industrially important systems; for example, alkanes of low molecular weight through to simple polymers[32,34] and their binary mixtures,[35–37] perfluoroalkanes,[38] hydrogen fluoride,[39] boron triflouride,[40] water,[41] refrigerant systems,[42] and carbon dioxide,[37,43] have all been studied. Additionally, a statistical associating fluid theory for potentials of variable range to model dipolar fluids[44] (SAFT-VR+D) was recently developed by the authors that explicitly accounts for dipolar interactions through the use of the generalized mean spherical approximation to describe a reference fluid of dipolar square-well segments.

Several variations of SAFT have been proposed to describe electrolyte solutions. For example, Liu *et al.*[45] established an EOS for aqueous electrolyte fluids based on Wertheim's theory for association interactions and the semirestricted NPMSA (i.e., equal sized hard spheres were used to model the cations and anions and a different sized hard sphere used for the solvent). Wu and Prausnitz[46] calculated the phase equilibria for systems containing hydrocarbons, water, and salt by combining the Peng-Robinson EOS with the SAFT term for association interactions and the MSA to describe the ion-ion interactions. Tan *et al.*[47] have coupled SAFT1 with the restricted primitive model (RPM) to represent aqueous strong electrolytes. Cameretti *et al.*[48] have extended the perturbed chain SAFT equation to model aqueous electrolyte solutions through the addition of a Debye-Hückel theory ion-ion interaction term. Of particular relevance is the work of Jackson and co-workers[49,50] who first extended the SAFT-VR EOS to model electrolyte solutions (SAFT-VRE) using an additive electrostatic term from the RPM with the MSA closure. The SAFT-VRE approach has been used to predict the vapor pressures of electrolyte solu-

tions in good agreement with experimental data; however, deviations from the experimental data are observed at high ion concentration ($>10M$), which may be due to the ion-solvent interactions not being adequately represented by the dielectric constant of the solvent. The SAFT-VRE approach has also been used to successfully study the salting out of *n*-alkanes in water by strong electrolytes[51] using the experimental dielectric constant for water as input to the calculations.

A common feature of these equations of state is that a MM level of theory is applied to describe the Coulombic interactions and therefore the effect of the solvent is not explicitly taken into account and values for the dielectric constant must be obtained. Here, building upon the SAFT-VR +D approach we present SAFT-VR+DE to model electrolyte solutions. The SAFT-VR+DE approach is a BO level equation of state that models electrolyte solutions through a combination of the MSA for the nonprimitive model and the statistical associating fluid theory for potentials of variable range (SAFT-VR); the nonprimitive model is used in order to explicitly take into account the effect of the solvent. *NPT* Monte Carlo simulations have been performed and used to validate the new approach. Additionally, to demonstrate the advantage of the use of the nonprimitive model, we compare results from the SAFT-VR approach and the nonprimitive model with those from the restricted nonprimitive model, which constrains the size of the cation, anion, and solvent to be equal, and the seminonprimitive model, in which only the ions and solvent are of different sizes with the size of the cation and anion being equal.

The remainder of the paper is organized as follows: In Sec. II we present the SAFT-VR+DE model and theory for electrolyte solutions. In Sec. III, details of the molecular simulations performed are presented. Results for the phase behavior of electrolyte solutions are presented and compared with simulation results in Sec. IV. Finally, concluding remarks are made and future work discussed in Sec. V.

## II. MODEL AND THEORY

In this work we develop a SAFT-VR approach to study the thermodynamic properties of electrolyte solutions in which the solvent is explicitly taken into account as a dipolar associating fluid. The electrolyte solutions are represented as a mixture of ions and solvent molecules. The ions are described as hard spheres, half with charge $+q$ and diameter $\sigma^+$, and half with charge $-q$ and diameter $\sigma^-$. The solvent is described as dipolar square-well molecules of diameter $\sigma_d$ with dipole moment $\mu$ embedded in the center of the molecule and four association sites to mimic the hydrogen bonding. As shown in Fig. 1, the four association sites, two of type *a* and two of type *b*, are situated off center at a distance $r_d$ in a tetrahedral arrangement on the hard sphere. Two sites of different types can interact through a square-well potential when they are closer than a distance $r_c$ apart. In our model for electrolyte solutions, in addition to the dispersion and association interactions between the solvent molecules, electrostatic charge-charge, charge-dipole, and dipole-dipole interactions describe the interaction of the ions, the interaction

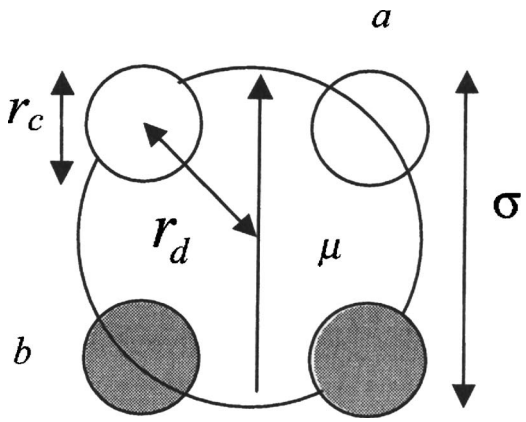


FIG. 1. Schematic model for the solvent molecule studied.

of the ions with the solvent, and the dipolar solvent-solvent interactions, respectively. Hence, the pair potential for the reference fluid is defined by

$$u(\mathbf{r}) = u^{\mathrm{SW}}(r) + u^{\mathrm{CC}}(r) + u^{\mathrm{CD}}(r) + u^{\mathrm{DD}}(r), \tag{2}$$

where $u^{\mathrm{SW}}(r)$ represents the square-well potential, $u^{\mathrm{CC}}(r)$ the Coulombic charge-charge interaction, $u^{\mathrm{CD}}(r)$ the charge-dipole interaction, and $u^{\mathrm{DD}}(r)$ the dipole-dipole interaction. The square-well potential is given by

$$u_{ij}^{\mathrm{SW}}(r) = \begin{cases} +\infty & \text{if } r < \sigma_{ij} \\ -\varepsilon_{ij} & \text{if } \sigma_{ij} \leqslant r < \lambda_{ij}\sigma_{ij} \\ 0 & \text{if } r \geqslant \lambda_{ij}\sigma_{ij}, \end{cases} \tag{3}$$

where $\sigma_{ij}$ is the diameter of the interaction, $\lambda_{ij}$ the range, and $\varepsilon_{ij}$ the depth of the square-well potential. The inter- and intramolecular cross interactions between segments are obtained from standard combining rules, viz.,

$$\sigma_{ij} = \frac{\sigma_{ii} + \sigma_{jj}}{2}, \tag{4}$$

$$\varepsilon_{ij} = (1 - k_{ij})(\varepsilon_{ii}\varepsilon_{jj})^{1/2}, \tag{5}$$

$$\lambda_{ij} = \left( \frac{\lambda_{ii}\sigma_{ii} + \lambda_{jj}\sigma_{jj}}{\sigma_{ii} + \sigma_{jj}} \right). \tag{6}$$

The Coulombic charge-charge potential between ions can be represented by

$$u_{ij}^{\mathrm{CC}}(r) = \begin{cases} +\infty & \text{if } r \leqslant \sigma_{ij} \\ z_i z_j e^2 / 4\pi\varepsilon r & \text{if } r > \sigma_{ij}, \end{cases} \tag{7}$$

where $r$ is the center-to-center distance, $e = 1.602 \times 10^{-19}$ C the elementary charge, and $\varepsilon$ the permittivity of the continuous dielectric medium. The charge-dipole potential can be defined by

$$u_{ij}^{\mathrm{CD}}(r) = \begin{cases} +\infty & \text{if } r \leqslant \sigma_{ij} \\ (z_i e \mu / 4\pi\varepsilon r^2)(\hat{r} \cdot \hat{n}) & \text{if } r > \sigma_{ij}, \end{cases} \tag{8}$$

and the dipole-dipole potential by

$$u_{ij}^{\mathrm{DD}}(r)=\begin{cases}+\infty & \text{if } r\leqslant\sigma_{ij}\\ -(\mu^2/4\pi\varepsilon r^3)D(\mathbf{n}_1\mathbf{n}_2\hat{\mathbf{r}}) & \text{if } r>\sigma_{ij},\end{cases} \tag{9}$$

where

$$D(\mathbf{n}_1\mathbf{n}_2\hat{\mathbf{r}})=3(\mathbf{n}_1\cdot\hat{\mathbf{r}})(\mathbf{n}_2\cdot\hat{\mathbf{r}})-\mathbf{n}_1\cdot\mathbf{n}_2. \tag{10}$$

Here $\hat{\mathbf{r}}$ is the unit vector in the direction of $\mathbf{r}$ joining the center of the segments and $\mathbf{n}_i$ is a unit vector parallel to the dipole moment of segment $i$.

Within the SAFT framework, the Helmholtz free energy $A$ for the electrolyte solutions studied in this work can be written in the form

$$\frac{A}{Nk_BT}=\frac{A^{\mathrm{ideal}}}{Nk_BT}+\frac{A^{\mathrm{mono}}}{Nk_BT}+\frac{A^{\mathrm{assoc}}}{Nk_BT}, \tag{11}$$

where $A^{\mathrm{ideal}}$ is the free energy of the ideal fluid, $A^{\mathrm{mono}}$ is the contribution due to the reference monomer fluid, and $A^{\mathrm{assoc}}$ represents the free energy due to association interactions. We have not included the contribution due to chain formation, as only charged/dipolar monomer molecules are considered in this initial study. We now present the general expressions for each term in Eq. (11) followed by the specific expressions for the ternary mixture of cations (component 1), anions (component 2), and solvent molecules (component 3) studied in this work.

### A. Ideal contribution

The ideal contribution to the free energy is expressed as

$$\frac{A^{\mathrm{ideal}}}{NkT}=\sum_{i=1}^{n}x_i\ln(\rho_i\Lambda_i^3)-1$$
$$=x_1\ln(\rho_1\Lambda_1^3)+x_2\ln(\rho_2\Lambda_2^3)+x_3\ln(\rho_3\Lambda_3^3)-1, \tag{12}$$

where $\rho_i=N_i/V$ is the number density, $\Lambda_i$ the thermal de Broglie wavelength of species $i$, and $x_i$ the mole fraction of component $i$.

### B. Monomer contribution

The monomer free energy is given by

$$\frac{A^{\mathrm{mono}}}{NkT}=\left(\sum_{x=1}^{n}x_im_i\right)\frac{A^{\mathrm{mono}}}{N_skT}=\left(\sum_{x=1}^{n}x_im_i\right)a^{\mathrm{mono}}, \tag{13}$$

where $N_s$ is the total number of segments, determined from the product of the total number of molecules $N$ and the number of segments per molecule $m_i$, which in this work is always equal to 1. $a^{\mathrm{mono}}$ is the free energy per monomer segment of the reference fluid which is a mixture of charged and dipolar hard spheres that interact through square-well and Coulombic charge-charge, charge-dipole, and dipole-dipole interactions. $a^{\mathrm{mono}}$ can be separated into two terms, $a^{\mathrm{SW}}$ due to the square-well potential and $a^{\mathrm{MSA}}$ due to the electrostatic interactions; hence,

$$a^{\mathrm{mono}}=a^{\mathrm{SW}}+a^{\mathrm{MSA}}. \tag{14}$$

In the SAFT-VR equation $a^{\mathrm{SW}}$ is approximated by a second order high temperature expansion using the perturbation theory for mixtures of Leonard *et al.*,[52] viz.,

$$a^{\mathrm{SW}}=a^{\mathrm{HS}}+\beta a_1+\beta a_2, \tag{15}$$

where $\beta=1/kT$, $a^{\mathrm{HS}}$ is the free energy of the hard-sphere reference fluid, and $a_1$ and $a_2$ are the first and second perturbation terms, respectively. The hard-sphere reference term is determined from the expression of Boublik[53] and Mansoori *et al.*[54] for multicomponent hard-sphere systems,

$$a^{\mathrm{HS}}=\frac{6}{\pi\rho_s}\left[\left(\frac{\zeta_2^3}{\zeta_3^2}-\zeta_0\right)\ln(1-\zeta_3)+\frac{3\zeta_1\zeta_2}{1-\zeta_3}+\frac{\zeta_2^3}{\zeta_3(1-\zeta_3)^2}\right], \tag{16}$$

where $\rho_s$ is the number density of segments, which is defined as the total number of segments divided by the total volume $(N_s/V)$, and $\zeta_l$ is the reduced density given by a sum over all segments $i$,

$$\zeta_l=\frac{\pi}{6}\rho_s\left[\sum_{i=1}^{n}x_{s,i}(\sigma_i)^l\right]$$
$$=\frac{\pi}{6}\rho_s[x_{s,1}(\sigma_1)^l+x_{s,2}(\sigma_2)^l+x_{s,3}(\sigma_3)^l], \tag{17}$$

where $\sigma_i$ is diameter of segments of type $i$ and $x_{s,i}$ is the mole fraction of segments in the mixture, and is given by

$$x_{s,i}=\frac{m_ix_i}{\sum_{k=1}^{n}m_kx_k}=\frac{m_ix_i}{m_1x_1+m_2x_2+m_3x_3}. \tag{18}$$

The first perturbation term $a_1$ describing the mean attractive energy is obtained from the sum of all pair interactions,

$$a_1=\sum_{i=1}^{n}\sum_{j=1}^{n}x_{s,i}x_{s,j}(a_1)_{ij}=x_{s,1}^2(a_1)_{11}+2x_{s,1}x_{s,2}(a_1)_{12}$$
$$+2x_{s,1}x_{s,3}(a_1)_{13}+x_{s,2}^2(a_1)_{22}+2x_{s,2}x_{s,3}(a_1)_{23}$$
$$+x_{s,3}^2(a_1)_{33}, \tag{19}$$

where $(a_1)_{ij}$ is obtained from the mean-value theorem as proposed by Gil-Villegas *et al.*,[32]

$$(a_1)_{ij}=-2\pi\rho_s\varepsilon_{ij}\int_{\sigma_{ij}}^{\infty}r_{ij}^2g_{ij}^{\mathrm{HS}}(r_{ij})dr_{ij}$$
$$=-\rho_s\alpha_{ij}^{\mathrm{VDW}}g_{ij}^{\mathrm{HS}}(\sigma_{ij};\zeta_3^{\mathrm{eff}}) \tag{20}$$

and

$$\alpha_{ij}^{\mathrm{VDW}}=\frac{2\pi}{3}\sigma_{ij}^3\varepsilon_{ij}(\lambda_{ij}^3-1). \tag{21}$$

In this work we use mixing rule MX3b as defined in Ref. 33 since we are concerned with the thermodynamics and phase behavior of electrolyte solutions and will not consider the critical region.[35] Therefore, $g_{ij}^{\mathrm{HS}}(\sigma_{ij};\zeta_3^{\mathrm{eff}})$ is given by

$$g_{ij}^{\mathrm{HS}}[\sigma_{ij};\zeta_3^{\mathrm{eff}}(\lambda_{ij})]=\frac{1}{(1-\zeta_3^{\mathrm{eff}})}+\frac{3D_{ij}\zeta_3^{\mathrm{eff}}}{(1-\zeta_3^{\mathrm{eff}})^2}+2\frac{(D_{ij}\zeta_3^{\mathrm{eff}})^2}{(1-\zeta_3^{\mathrm{eff}})^3}, \tag{22}$$

where $D_{ij}$ is given by

$$D_{ij} = \frac{\sigma_{ii}\sigma_{jj}}{\sigma_{ii}+\sigma_{jj}} \frac{\Sigma_{i=1}^{n} x_i \sigma_{ii}^2}{\Sigma_{i=1}^{n} x_i \sigma_{ii}^3}. \tag{23}$$

The effective packing fraction $\zeta_3^{\text{eff}}(\lambda_{ij})$ can be written as

$$\zeta_3^{\text{eff}}(\zeta_3,\lambda_{ij}) = c_1(\lambda_{ij})\zeta_3 + c_2(\lambda_{ij})\zeta_3^2 + c_3(\lambda_{ij})\zeta_3^3, \tag{24}$$

and following the original SAFT-VR approach,[33]

$$\begin{pmatrix} c_1 \\ c_2 \\ c_3 \end{pmatrix} = \begin{pmatrix} 2.258\,55 & -1.503\,49 & 0.249\,434 \\ -0.669\,270 & 1.400\,49 & -0.827\,739 \\ 10.1576 & -15.0427 & 5.308\,27 \end{pmatrix} \begin{pmatrix} 1 \\ \lambda_{ij} \\ \lambda_{ij}^2 \end{pmatrix}. \tag{25}$$

The second order perturbation term for the monomer excess free energy $a_2$ is expressed as

$$\begin{aligned} a_2 &= \sum_{i=1}^{n}\sum_{j=1}^{n} x_{s,i}x_{s,j}(a_2)_{ij} \\ &= x_{s,1}^2(a_2)_{11} + 2x_{s,1}x_{s,2}(a_2)_{12} + 2x_{s,1}x_{s,3}(a_2)_{13} \\ &\quad + x_{s,2}^2(a_2)_{22} + 2x_{s,2}x_{s,3}(a_2)_{23} + x_{s,3}^2(a_2)_{33}, \end{aligned} \tag{26}$$

where $(a_2)_{ij}$ is obtained through the local compressibility approximation:

$$(a_2)_{ij} = \frac{1}{2}K^{\text{HS}}\varepsilon_{ij}\rho_s \frac{\partial(a_1)_{ij}}{\partial\rho_s}, \tag{27}$$

where $K^{\text{HS}}$ is the Percus-Yevick expression for the hard-sphere isothermal compressibility,

$$K^{\text{HS}} = \frac{\zeta_0(1-\zeta_3)^4}{\zeta_0(1-\zeta_3)^2 + 6\zeta_1\zeta_2(1-\zeta_3) + 9\zeta_2^3}. \tag{28}$$

For the contribution to the free energy due to the electrostatic interactions, $a^{\text{MSA}}$, we use the nonprimitive model in order to explicitly take into account the effect of the solvent. Recognizing the inconstancies reported in the literature for the expressions of Wei and Blum's solution for the nonprimitive model within the mean spherical approximation, here we briefly summarize the expressions used in this work;[55] the expressions for the other models considered for comparison are listed in the Appendix. In the MSA, the properties for the nonprimitive model are expressible with three parameters, $\Gamma$, $B_{10}$, and $b_2$, which correspond to the ion-ion, ion-dipole, and dipole-dipole interactions, respectively, and are given by the solution of three algebraic equations, viz.,

$$\sum_{i=1}^{n-1} \rho_i (a_i^0)^2 + \rho_n (a_n^1)^2 = \alpha_0^2, \tag{29}$$

$$-\sum_{i=1}^{n-1} \rho_i a_i^0 k_{ni}^{10} + a_n^1(1-\rho_n k_{nm}^{11}) = \alpha_0\alpha_2, \tag{30}$$

$$(1-\rho_n k_{nm}^{11})^2 + \rho_n \sum_{i=1}^{n-1} \rho_i (k_{ni}^{10})^2 = y_1^2 + \rho_n\alpha_2^2, \tag{31}$$

where the quantities in Eqs. (29)–(31) are defined as

$$\begin{aligned} &\alpha_0^2 = 4\pi\beta e^2, \quad \alpha_2^2 = \frac{4\pi\beta\mu^2}{3}, \\ &\beta_3 = 1 + \tfrac{1}{3}b_2, \quad \beta_6 = 1 - \tfrac{1}{6}b_2, \\ &\lambda = \frac{\beta_3}{\beta_6}, \quad y_1 = \frac{4}{\beta_6(1+\lambda)^2}, \\ &w_1 = \sum_{i=1}^{n-1} \frac{\rho_i z_i^2}{\beta_6(\sigma_n+\lambda\sigma_i)(1+\Gamma\sigma_i)}, \\ &w_2 = \frac{1}{2}\rho_n\sigma_n^2 B_{10} \sum_{i=1}^{n-1} \frac{\rho_i z_i^2 \sigma_i^2}{[2\beta_6(\sigma_n+\lambda\sigma_i)(1+\Gamma\sigma_i)]^2}, \\ &\upsilon_\eta = \frac{-w_1/2 + \sqrt{(w_1/2)^2 + 2B_{10}w_2/\beta_6^2}}{w_2}, \\ &\Delta\Gamma_i = \frac{\upsilon_\eta\rho_n\sigma_n^2\sigma_i^2 B_{10}}{8\beta_6(\sigma_n+\lambda\sigma_i)}, \\ &D_i^F = \frac{z_i\beta_6}{2(1+\sigma_i\Gamma-\Delta\Gamma_i)}, \quad m_i = \frac{\upsilon_\eta D_i^F}{(\sigma_n+\lambda\sigma_i)}, \\ &D = 1 + \upsilon_\eta^2\rho_n\sigma_n^2 \sum_{i=1}^{n-1} \frac{\rho_i\sigma_i^2(D_i^F)^2}{[2\beta_6(\sigma_n+\lambda\sigma_i)]^2}, \quad D_{ac} = \sum_{i=1}^{n-1} \rho_i (D_i^F)^2, \\ &\Gamma_i^s = \frac{(1+\Gamma\sigma_i-\Delta\Gamma_i)D-1}{\sigma_i}, \\ &\Omega_{10} = \upsilon_\eta \sum_{i=1}^{n-1} \frac{\rho_i\sigma_i(D_i^F)^2}{(\sigma_n+\lambda\sigma_i)}, \\ &N_i = \frac{2D_i^F}{\beta_6\sigma_i}\left[1 + \frac{\upsilon_\eta\rho_n\sigma_n^3 B_{10}\sigma_i}{24(\sigma_n+\lambda\sigma_i)}\right] - \frac{z_i}{\sigma_i}, \\ &a_i^0 = \frac{\beta_6\Gamma_i^s D_i^F}{D_{ac}}, \quad a_n^1 = \frac{D\beta_6}{2D_{ac}}\left[\frac{\sigma_n B_{10}}{2} + \frac{\Omega_{10}\lambda}{D\beta_6}\right], \\ &-k_{ni}^{10} = \frac{\sigma_n^2 D_i^F}{2D\beta_6^2}\left[\frac{\upsilon_\eta}{(\sigma_n+\lambda\sigma_i)} + \frac{\Omega_{10}\Gamma_i^s}{D_{ac}}\right] + \frac{\sigma_n^3 B_{10} a_i^0}{12\beta_6}, \\ &1-\rho_n k_{nm}^{11} = \frac{1}{D\beta_6}\left[\lambda + \frac{\rho_n\sigma_n^2\Omega_{10}a_n^1}{2\beta_6^2}\right] + \frac{\rho_n\sigma_n^3 B_{10}a_n^1}{12\beta_6}. \end{aligned} \tag{32}$$

In the mean spherical approximation, the excess internal energy is given by[55]

$$\frac{\beta E}{V} = \frac{1}{4\pi}\left\{\alpha_0^2 \sum_{i=1}^{n-1} \frac{\rho_i z_i^2 (D-1-\sigma_i\Gamma_i^s)}{\sigma_i(1+\sigma_i\Gamma_i^s)} - \rho_n\alpha_0 B_{10}\left(\frac{-B_{10}\sigma_n^3 a_0}{12\beta_6} + 2\alpha_2\right) - \frac{2\alpha_2^2\rho_n b_2}{\sigma_n^3}\right\}, \tag{34}$$

and the ionic excess chemical potentials is given by

$$\beta\mu_i = \frac{z_i(\alpha_0^2 N_i - \alpha_0\alpha_2\rho_n m_i)}{4\pi}. \tag{35}$$

The chemical potential of dipolar molecules is given by

$$\beta\mu_n = \frac{(-\alpha_0\alpha_2 B_{10} - 2\alpha_2^2 b_2/\sigma_n^3)}{4\pi}. \tag{36}$$

Following Adelman[56] the dielectric constant can be written as

$$\varepsilon_A = 1 + \frac{\rho_n\alpha_2^2\beta_6^2(1+\lambda)^4}{16}. \tag{37}$$

The excess Helmholtz free energy is given by[55]

$$\frac{\beta A}{V} = \frac{1}{12\pi}\left\{-2\alpha_0^2\sum_{i=1}^{n-1}\frac{\rho_i z_i^2(D-1-\sigma_i\Gamma_i^s)}{\sigma_i(1+\sigma_i\Gamma_i^s)} + \rho_n\alpha_0 B_{10}\left(\frac{-B_{10}\sigma_n^3\alpha_0}{12\beta_6} + 2\alpha_2\right)\right\} + J', \tag{38}$$

where

$$J' = \frac{1}{3\pi}\sum_{mnl}\sum_{ij}\rho_i\rho_j\sigma_{ij}^3(2l+1)^{-1}[h_{ij}^{mnl}(r=\sigma_{ij})]^2,$$

$$h_{ij}^{000}(\sigma_{ij}) = \frac{Q_{ij}'^{00}}{3\pi\sigma_{ij}},$$

$$h_{in}^{011}(\sigma_{in}) = \frac{\sqrt{3}Q_{in}'^{01}}{3\pi\sigma_{in}}, \tag{39}$$

$$h_{nn}^{110}(\sigma_n) = \frac{Q_{nn}'^{11} + 2q'}{2\sqrt{3}\pi\sigma_n},$$

$$h_{nn}^{112}(\sigma_n) = \frac{\sqrt{10}(Q_{nn}'^{11} - q')}{2\sqrt{3}\pi\sigma_n},$$

and where

$$q' = \frac{-b_2(\lambda+3)}{(1+\lambda)^2},$$

$$Q_{ij}'^{00} = \frac{2\pi}{\Delta}\left(\sigma_{ij} + \frac{\pi\sigma_i\sigma_j\xi_2}{4\Delta}\right) - \frac{1}{2}D_i^F D_j^F\left(\frac{\rho_n\sigma_n^2\upsilon_\eta^2}{D\beta_6^2(\sigma_n+\lambda\sigma_i)(\sigma_n+\lambda\sigma_j)} + \frac{4\Gamma_i^s\Gamma_j^s}{DD_{ac}}\right),$$

$$Q_{in}'^{00} = Q_{ni}'^{00} = \frac{2\pi}{\Delta}\left(\sigma_{in} + \frac{\pi\sigma_i\sigma_n\xi_2}{4\Delta}\right), \tag{40}$$

$$Q_{in}'^{01} = -\frac{D_i^F}{D\beta_6}\left(\frac{\lambda\upsilon_\eta}{\sigma_n+\lambda\sigma_i} + 2\Gamma_i^s a_n^1\right),$$

$$Q_{ni}'^{10} = \frac{D_i^F}{D\beta_6}\left(\frac{\lambda\upsilon_\eta}{\sigma_n+\lambda\sigma_i} + 2\Gamma_i^s a_n^1\right),$$

$$Q_{nn}'^{11} = \frac{2\lambda}{D\rho_n\sigma_n^2}\left(\lambda + \frac{\rho_n\sigma_n^2\Omega^{10}a_n^1}{2\beta_6^2}\right) + \frac{\sigma_n B_{10}a_n^1}{2\beta_6} - \frac{2}{\rho_n\sigma_n^2}.$$

Since in the MSA the excess Gibbs free energy equals the excess internal energy, the pressure is given by

$$\beta P = \frac{\beta(E-A)}{V}. \tag{41}$$

### C. Association contribution

Based on the theory of Wertheim, the contribution due to association of $s_i$ sites on species $i$ is obtained as[57]

$$\frac{A^{\text{assoc}}}{NkT} = \sum_{i=1}^{n} x_i\left[\sum_{a=1}^{s_i}\left(\ln X_{a,i} - \frac{X_{a,i}}{2}\right) + \frac{s_i}{2}\right], \tag{42}$$

where the first sum is over the number of species $i$ and the second sum is over all $s_i$ sites of type $a$ on species $i$, and $X_{a,i}$ is the fraction of molecules of type $i$ not bonded at site $a$, which is obtained from the numerical solution of the mass action equation:

$$X_{a,i} = \frac{1}{1 + \sum_{j=1}^{n}\sum_{b=1}^{s_i}\rho x_j X_{b,j}\Delta_{a,b,i,j}}. \tag{43}$$

The function $\Delta_{a,b,i,j}$, which characterizes the association between site $a$ on molecule $i$ and site $b$ on molecules $j$, can be written as

$$\Delta_{a,b,i,j} = K_{a,b,i,j}f_{a,b,i,j}g_{ij}^{\text{SW}}(\sigma_{ij};\zeta_3), \tag{44}$$

where $f_{a,b,i,j}=\exp(-\psi_{a,b,i,j}/kT)-1$ is the Mayer $f$ function of the $a$-$b$ site-site bonding interaction $\psi_{a,b,i,j}$, and $K_{a,b,i,j}$ is the volume available for bonding.[58] As in the original SAFT-VR approach the radial distribution $g_{ij}^{\text{sw}}$ function is obtained as

$$g_{ij}^{\text{SW}}(\sigma_{ij};\zeta_3) = g_0^{\text{HS}}(\sigma_{ij};\zeta_3) + \beta\varepsilon_{ij}g_1(\sigma_{ij};\zeta_3), \tag{45}$$

where the hard-sphere radial distribution function is given by Eq. (22) and $g_1(\sigma_{ij};\zeta_3)$ is given by

$$g_1(\sigma_{ij};\zeta_3) = \frac{1}{2\pi\varepsilon_{ij}\sigma_{ij}^3}\left[3\left(\frac{\partial a_1^{ij}}{\partial\rho_s}\right) - \frac{\lambda_{ij}}{\rho_s}\frac{\partial a_1^{ij}}{\partial\lambda_{ij}}\right]. \tag{46}$$

In our model for electrolyte solutions only the solvent molecules are modeled as associating molecules, each having four association sites. Therefore, the association contribution to the free energy for a fluid with a four-site associating component can be simplified from Eq. (42) to

$$\frac{A^{\text{assoc}}}{NkT} = x_3\left[4\left(\ln X_3 - \frac{X_3}{2}\right) + 2\right], \tag{47}$$

and since all four sites are equivalent the fraction of solvent molecules not bonded is given by

$$X_3 = \frac{1}{1 + 2\rho x_3 X_3\Delta_{33}}, \tag{48}$$

where $\Delta_{33}$ is defined by Eq. (44).

TABLE I. Model parameters for the electrolyte fluids studied. $\sigma_d^*$ is the reduced diameter of the solvent molecules, $\sigma^{+*}$ and $\sigma^{-*}$ the reduced diameters of the cation and anion, respectively, $\mu^{*2}$ the solvent reduced dipole moment ($\mu^{*2}=\mu^2/4\pi\varepsilon_0 k_B \varepsilon \sigma^3$), $\varepsilon^*$ the reduced depth of the square-well potential, λ the range of the potential, $\psi^*$ the reduced association energy, $r_c^*$ the reduced association cutoff radius, $N^{\text{ion}}$ the number of ions, and $N^{\text{solvent}}$ the number of solvent molecules.

| System | $\sigma_d^*$ | $\sigma^{+*}$ | $\sigma^{-*}$ | $\mu^{*2}$ | $\varepsilon^*$ | λ | $\psi^*$ | $r_c^*$ | $N^{\text{ion}}$ | $N^{\text{solvent}}$ |
|---|---|---|---|---|---|---|---|---|---|---|
| 1 | 1 | 1 | 1 | 0.5 | 1 | 1.5 | 5 | 1.05 | 8 | 248 |
| 2 | 1 | 1 | 1 | 1.0 | 1 | 1.5 | 5 | 1.05 | 8 | 248 |
| 3 | 1 | 1 | 1 | 0.5 | 1 | 1.5 | 5 | 1.05 | 4 | 252 |
| 4 | 1 | 1 | 1 | 0.5 | 1 | 1.5 | 5 | 1.05 | 16 | 240 |
| 5 | 1 | 0.5 | 0.5 | 1.0 | 1 | 1.5 | 5 | 1.05 | 8 | 248 |
| 6 | 1 | 1/3 | 2/3 | 1.0 | 1 | 1.5 | 5 | 1.05 | 8 | 248 |

## III. COMPUTER SIMULATIONS

Monte Carlo (MC) simulations have been performed to study the thermodynamic properties of several model electrolyte solutions and provide data with which to test the new theoretical approach. The simulations were performed in the isothermal-isobaric (*NPT*) ensemble. The reaction field (RF) method, which truncates the potential at a finite distance from each ion and dipolar molecule, was used to describe the long-range charge-charge, charge-dipole, and dipole-dipole interactions.[59] The reaction field approach replaces the molecules beyond the cutoff distance by a dielectric continuum, the effect of which is taken into account by including an additional term into the long-range charge-charge, charge-dipole, and dipole-dipole interactions, viz.,

$$u^{\text{CC}} = \begin{cases} q_i q_j [1/r + ((\varepsilon_{\text{RF}} - 1)/(2\varepsilon_{\text{RF}} + 1))(r^2/r_c^3)], & r < r_c \\ 0, & r \geqslant r_c, \end{cases} \tag{49}$$

$$u^{\text{CD}} = \begin{cases} (2(\varepsilon_{\text{RF}} - 1)/(2\varepsilon_{\text{RF}} + 1))(r/r_c^3) q \cdot \mu, & r < r_c \\ 0, & r \geqslant r_c, \end{cases} \tag{50}$$

$$u^{\text{DD}} = \begin{cases} -(\mu_1 \mu_2 / r^3) D - (2(\varepsilon_{\text{RF}} - 1)/(2\varepsilon_{\text{RF}} + 1))(\mu_1 \mu_2 / r_c^3), & r < r_c \\ 0, & r \geqslant r_c, \end{cases} \tag{51}$$

where $r_c$ is the cutoff distance beyond which the pair potential is set to zero and $\varepsilon_{\text{RF}}$ the dielectric constant of the continuum. In our simulations, the value of $r_c$ is set to $3.0\sigma$ and $\varepsilon_{\text{RF}}$ to ∞. The usual periodic boundary conditions and minimum image convention are used. One simulation cycle consists of three kinds of trial moves: $N$ trial displacements of randomly chosen molecules, $N$ trial rotations, and one volume change. The extent of each trial move is adjusted to give an individual acceptance probability of 30%–40%. Each simulation was started from an initial configuration in which 256 molecules are placed on a lattice in the simulation box. An initial simulation of 100 000–500 000 cycles was performed to equilibrate the system, before averaging for between 500 000 and 1 000 000 cycles. The thermodynamic properties of the system were obtained as ensemble averages and the errors estimated by determining the standard deviation.

## IV. RESULTS AND DISCUSSION

We have studied the *PVT* behavior of several model electrolyte solutions. In particular, comparisons are made between theoretical predictions and *NPT* ensemble Monte Carlo simulation data for several model systems in order to test the new SAFT-VR+DE approach. The ability of the SAFT-VR+D equation to accurately predict the effect of the strength of the dipole moment and dispersion interactions on the thermodynamics of fluids was verified in previous work.[44] The model systems studied in this work therefore focus on the effect of the ability of the new theoretical approach to capture the effect of the ions and are detailed in Table I. From Table I, systems 1–4 are restricted electrolyte solution models, in that they have equal sized ions and solvent molecules; system 5 represents a semisymmetric electrolyte solution in which the ions are of equal size, but differ from the size of the solvent; and system 6 describes an asymmetric electrolyte solution with different sized cation, anion, and solvent molecules. The results of the *NPT* Monte Carlo simulations are reported in Tables II and III.

In Fig. 2, we present a comparison between predictions from the SAFT-VR+DE approach and the *NPT* ensemble

TABLE II. *NPT* MC simulation results for systems 1–4. The reduced temperature is given by $T^*=k_BT/\varepsilon$, the reduced pressure by $P^*=P\sigma^3/\varepsilon$, and the reduced energy by $E^*=E/N\varepsilon$.

| System | $T^*$ | $P^*$ | $\eta$ | *Error* | $-E^*$ | *Error* |
|---|---|---|---|---|---|---|
| 1 | 1.2 | 0.3208 | 0.402 | 0.008 | 17.47 | 0.28 |
| | | 2.1922 | 0.451 | 0.005 | 19.20 | 0.23 |
| | 1.4 | 0.4548 | 0.357 | 0.008 | 15.26 | 0.25 |
| | | 1.6788 | 0.402 | 0.007 | 16.31 | 0.33 |
| | | 4.2295 | 0.447 | 0.006 | 17.11 | 0.23 |
| | 1.6 | 1.2669 | 0.353 | 0.007 | 14.70 | 0.22 |
| | | 2.9478 | 0.401 | 0.005 | 15.33 | 0.20 |
| | | 6.1674 | 0.451 | 0.006 | 16.46 | 0.22 |
| | 1.8 | 0.9596 | 0.294 | 0.008 | 13.37 | 0.50 |
| | | 2.0401 | 0.352 | 0.014 | 13.92 | 0.80 |
| | | 4.1532 | 0.398 | 0.012 | 14.64 | 0.70 |
| | | 8.0221 | 0.450 | 0.015 | 16.57 | 0.73 |
| 2 | 1.2 | 0.1859 | 0.411 | 0.008 | 18.96 | 0.42 |
| | | 2.0379 | 0.452 | 0.004 | 19.93 | 0.22 |
| | 1.4 | 0.3421 | 0.359 | 0.007 | 16.48 | 0.24 |
| | | 1.5471 | 0.406 | 0.006 | 17.82 | 0.27 |
| | | 4.0785 | 0.454 | 0.004 | 18.80 | 0.22 |
| | 1.6 | 0.3773 | 0.295 | 0.009 | 14.03 | 0.23 |
| | | 1.1570 | 0.353 | 0.008 | 15.19 | 0.24 |
| | | 2.8190 | 0.408 | 0.005 | 17.34 | 0.21 |
| | | 6.0196 | 0.452 | 0.005 | 17.94 | 0.23 |
| | 1.8 | 0.8709 | 0.299 | 0.007 | 13.64 | 0.20 |
| | | 1.9329 | 0.357 | 0.007 | 14.814 | 0.22 |
| | | 4.0273 | 0.405 | 0.006 | 16.50 | 0.32 |
| | | 7.8772 | 0.453 | 0.005 | 17.39 | 0.21 |
| 3 | 1.2 | 0.4974 | 0.3982 | 0.0059 | 12.15 | 0.24 |
| | | 2.3668 | 0.4458 | 0.0064 | 13.40 | 0.25 |
| | 1.4 | 0.6295 | 0.3508 | 0.0068 | 10.06 | 0.23 |
| | | 1.8628 | 0.3996 | 0.0061 | 11.19 | 0.22 |
| | | 4.4158 | 0.4472 | 0.0048 | 12.33 | 0.22 |
| | 1.6 | 0.6315 | 0.3068 | 0.0080 | 8.59 | 0.21 |
| | | 1.4475 | 0.3513 | 0.0067 | 9.48 | 0.21 |
| | | 3.1401 | 0.4012 | 0.0061 | 10.57 | 0.21 |
| | | 6.3641 | 0.4464 | 0.0049 | 11.58 | 0.21 |
| | 1.8 | 1.1258 | 0.3041 | 0.0078 | 8.19 | 0.20 |
| | | 2.2254 | 0.3504 | 0.0066 | 9.08 | 0.19 |
| | | 4.3522 | 0.4002 | 0.0054 | 10.11 | 0.19 |
| | | 8.2274 | 0.4470 | 0.0039 | 11.08 | 0.18 |
| 4 | 1.2 | 0.5878 | 0.419 | 0.005 | 29.77 | 0.22 |
| | | 1.8917 | 0.456 | 0.003 | 30.40 | 0.20 |
| | 1.4 | 0.1432 | 0.348 | 0.004 | 25.35 | 0.19 |
| | | 1.3541 | 0.405 | 0.004 | 28.39 | 0.21 |
| | | 3.9055 | 0.457 | 0.004 | 30.47 | 0.21 |
| | 1.6 | 0.1738 | 0.318 | 0.011 | 22.61 | 0.80 |
| | | 0.9429 | 0.350 | 0.009 | 24.70 | 0.35 |
| | | 2.6061 | 0.406 | 0.005 | 27.74 | 0.20 |
| | | 5.8224 | 0.458 | 0.004 | 29.72 | 0.20 |
| | 1.8 | 0.6583 | 0.292 | 0.009 | 21.44 | 0.73 |
| | | 1.7062 | 0.357 | 0.01 | 25.99 | 1.59 |
| | | 3.7977 | 0.404 | 0.005 | 27.23 | 0.20 |
| | | 7.6592 | 0.457 | 0.006 | 28.19 | 0.46 |

simulation results for the *PVT* behavior of the model restricted electrolyte solution in which the cation, anion, and solvent molecules are all of the same size (i.e., systems 1 and 2). Two different dipolar solvents are considered: system 1 with $\mu^{*2}=0.5$ and system 2 with $\mu^{*2}=1.0$. From Fig. 2 we see that good agreement between the simulation results and theoretical predictions over a wide range of temperatures and pressures is observed, though the proposed approach is seen to slightly underpredict the simulation data at high densities. This could be due to inadequate sampling in the Monte Carlo

TABLE III. *NPT* MC simulation results for systems 5 and 6. The reduced temperature is given by $T^*=k_BT/\varepsilon$, the reduced pressure by $P^*=P\sigma^3/\varepsilon$, and the reduced energy by $E^*=E/N\varepsilon$.

| System | $T^*$ | $P^*$ | $\eta$ | *Error* | $-E^*$ | *Error* |
|---|---|---|---|---|---|---|
| 5 | 1.4 | 0.0724 | 0.334 | 0.010 | 18.95 | 0.29 |
| | | 1.1905 | 0.395 | 0.005 | 20.40 | 0.30 |
| | | 3.6384 | 0.446 | 0.006 | 21.12 | 0.24 |
| | 1.6 | 0.2337 | 0.279 | 0.005 | 16.68 | 0.19 |
| | | 0.9472 | 0.338 | 0.005 | 18.67 | 0.20 |
| | | 2.5400 | 0.396 | 0.006 | 19.54 | 0.23 |
| | | 5.6772 | 0.448 | 0.006 | 20.30 | 0.23 |
| | 1.8 | 0.7658 | 0.285 | 0.005 | 16.17 | 0.29 |
| | | 1.7745 | 0.347 | 0.005 | 18.01 | 0.19 |
| | | 3.8157 | 0.397 | 0.005 | 19.09 | 0.20 |
| | | 7.6213 | 0.450 | 0.005 | 19.73 | 0.21 |
| 6 | 1.4 | 0.0656 | 0.350 | 0.003 | 19.65 | 0.20 |
| | | 1.1802 | 0.391 | 0.007 | 19.82 | 0.25 |
| | | 3.6225 | 0.442 | 0.005 | 20.35 | 0.42 |
| | 1.6 | 0.2289 | 0.306 | 0.015 | 17.26 | 0.33 |
| | | 0.9399 | 0.343 | 0.007 | 17.30 | 0.29 |
| | | 2.5288 | 0.399 | 0.006 | 19.24 | 0.22 |
| | | 5.6596 | 0.444 | 0.005 | 19.59 | 0.33 |
| | 1.8 | 0.7607 | 0.302 | 0.007 | 16.29 | 0.40 |
| | | 1.7666 | 0.356 | 0.005 | 17.31 | 0.66 |
| | | 3.8033 | 0.398 | 0.006 | 18.68 | 0.21 |
| | | 7.6018 | 0.446 | 0.006 | 18.91 | 0.36 |

simulations at high densities due to association interactions;[60] a similar trend was observed in a recent study of dipolar associating systems.[61]

Since the concentration of ions in electrolyte solutions plays an important role in determining their thermodynamic properties, we have studied the *PVT* behavior of electrolyte solutions with differing ion concentrations, namely, 0.79%, 1.59%, and 3.2% which correspond to systems 1, 3, and 4, respectively. The concentrations reported are in the form of mol % of salt; for comparison, a 1*M* NaCl solution corresponds to 1.77 mol %. The results for systems 3 and 4 are presented in Fig. 3. From Figs. 2 and 3 we note that good agreement is obtained in all cases between the simulation data and theoretical predictions for the systems studied and that as the concentration of the ions increases the density at a given pressure and temperature increases, due to the increased attractive interaction, which at constant density would result in reduced pressure, and so at constant pressure results in the increase of density.

In order to obtain a more comprehensive understanding of the thermodynamic properties of the systems studied, we have also examined different models for incorporating the long-range interactions, namely, the Debye-Hückel theory and the primitive and nonprimitive models. In Fig. 4, we present a comparison of the theoretical predictions from these different electrolyte models, with the results from the SAFT-VR+DE approach and the *NPT* ensemble MC simulation data for system 2. The results are presented at a single temperature, $T^*=1.8$, for clarity. As mentioned previously, for the Debye-Hückel theory and the primitive models, we need to predetermine the dielectric constant of the dipolar solvent, which depends on the dipole moment, temperature, and the composition of the electrolyte solution. In applications of the primitive model the determination of the dielectric constant can be problematic and often introduces additional approximations. For example, in the SAFT-VRE approach,[49] the experimental value of the dielectric constant of pure water at each temperature is typically used in the study of aqueous electrolyte solutions, while Wu and Prausnitz[46] in their work proposed a correlation for the dielectric constant of mixtures of hydrocarbons and aqueous salt solution based on the dielectric constant of water, the composition of the mixture, and an adjustable constant for each hydrocarbon. In the SAFT-VR+DE approach the dielectric constant is not required as an input to the calculations. However, in order to compare different models for incorporating the long-range interactions we must determine the dielectric constant for the Debye-Hückel and primitive models. Since dielectric constant data are not available for model solutions, we calculate the dielectric constant using Adelman's formula for the nonprimitive model. We see from Fig. 4 that the theoretical prediction from the SAFT-VR approach with Debye-Hückel theory greatly overpredicts the density at a given pressure and temperature due to the exclusion of the effect of the volume of the ions, while the theoretical predictions from the primitive models underpredict the density at given pressure and temperature, with the RPM and PM yielding identical predictions (since the system studied is symmetric). The prediction from the SAFT-VR+DE approach (i.e., nonprimitive model) is in excellent agreement with the simulation data, illustrating the need for an accurate ion-concentration-dependent dielectric constant. As expected for the symmetric system studied the restricted nonprimitive model and the seminonprimitive model provide the same so-

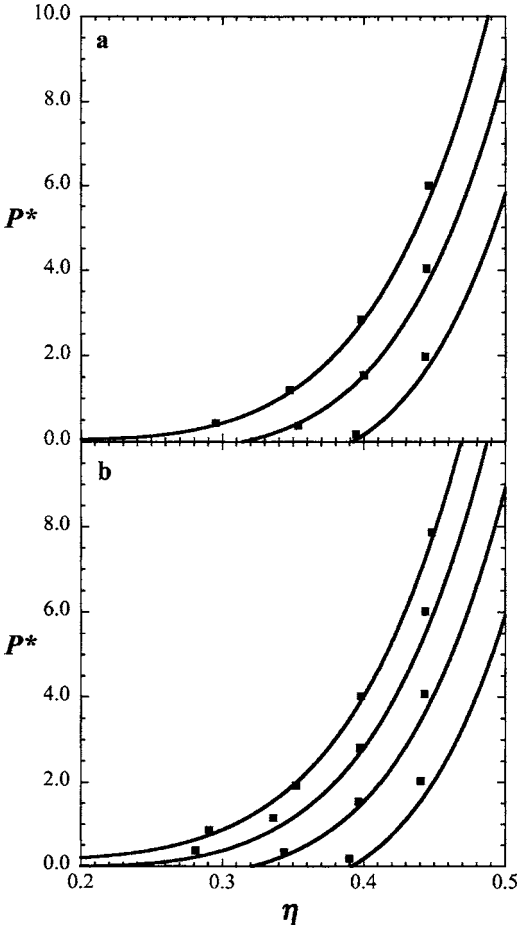


FIG. 2. Comparison of predictions from the SAFT-VR+DE approach and *NPT* MC simulation data for symmetric electrolyte solutions with $\varepsilon^*=1.0$, $\lambda=1.5$, $\sigma^{+*}=\sigma^{-*}=\sigma_d^*=1.0$, $\psi^*=5.0$, $r_c^*=1.05$, charge $q=1$, ion concentration of 8/256, and (a) dipole moment $\mu^{*2}=0.5$ at $T^*=1.2$, 1.4, and 1.6 (from bottom to top) for system 1 and (b) dipole moment $\mu^{*2}=1.0$ at $T^*=1.2$, 1.4, 1.6, and 1.8 (from bottom to top) for system 2. The solid lines represent predictions from the SAFT-VR+DE equation and the squares the *NPT* MC simulation data.

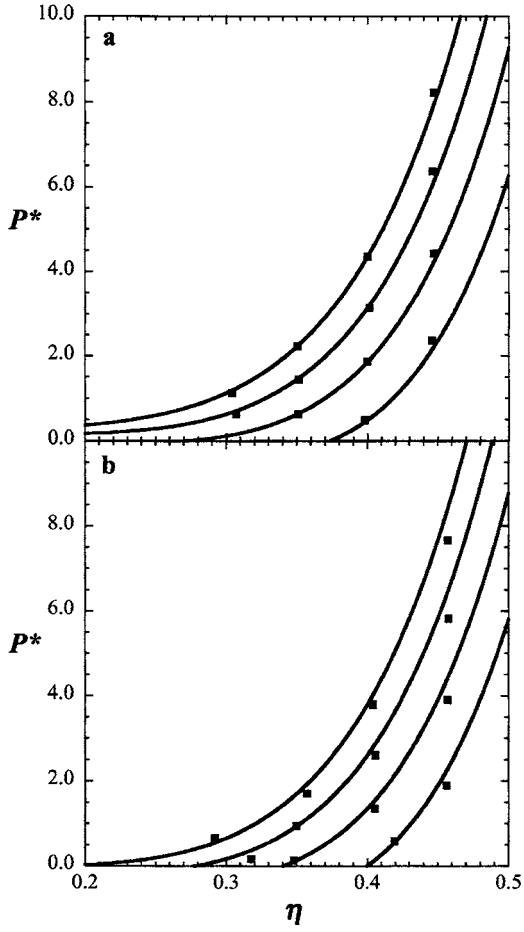


FIG. 3. Comparison of predictions from the SAFT-VR+DE approach and *NPT* MC simulation data for symmetric electrolyte solutions with $\varepsilon^*=1.0$, $\lambda=1.5$, $\sigma^{+*}=\sigma^{-*}=\sigma_d^*=1.0$, $\psi^*=5.0$, $r_c^*=1.05$, charge $q=1$, dipole moment $\mu^{*2}=0.5$, and ion concentrations of (a) 4/256 at $T^*=1.2$, 1.4, 1.6, and 1.8 (from bottom to top) for system 3 and (b) 16/256 at $T^*=1.2$, 1.4, 1.6, and 1.8 (from bottom to top) for system 4. The solid lines represent predictions from the SAFT-VR+DE equation and the squares the *NPT* MC simulation data.

lutions. We note that the relatively good agreement obtained between the simulation data and primitive models can be attributed to the use of the dielectric constant from the nonprimitive model in the calculations.

Having seen that the SAFT-VR+DE equation with the nonprimitive model to describe the long-range interactions can accurately describe the *PVT* behavior of symmetric electrolyte solutions, we now turn to semisymmetric electrolyte solutions, which have ions of the same size but different sized solvent molecules. In Fig. 5 we present the *PVT* behavior for a semisymmetric electrolyte solution (system 5), which has the same model parameters as system 2 but the size of the ions is now half that of the solvent. From the figures (Figs. 5 and 2), we find that the semisymmetric electrolyte solution exhibits a slightly higher density at a given pressure and temperature than the symmetric electrolyte solution [Fig. 2(b)] and that the SAFT-VR+DE EOS provides good agreement with the simulation data for the isotherms studied. In order to demonstrate the advantages and accuracy of the SAFT-VR+DE approach and the difference between the nonprimitive model and other MSA models for the long-range electrostatic interactions, we have again compared the isotherms predicted from the SAFT-VR+DE approach with predictions from the SAFT-VR approach combined with the Debye-Hückel theory and the primitive model (RPM and PM). The results from the different models studied for system 5 at $T^*=1.8$ are shown in Fig. 6, along with the *NPT* ensemble MC simulation data for comparison. It can be seen from the figure that the predictions using Debye-Hückel theory show the greatest deviations from the simulation data. The results from the primitive models and the restricted nonprimitive model consistently underestimate the density, which again illustrates the need for an accurate ion-concentration-dependent dielectric constant and the importance of correctly accounting for the effect of the size of the ions and solvent. The results using the RPM and PM model both underpredict the density at given temperature and pressure and result in identical predictions since both models do not explicitly take into account the solvent but mimic the solvent as a dielectric continuum. We again note that the apparent good agreement obtained between the simulation data and primitive models is due to the use of the dielectric

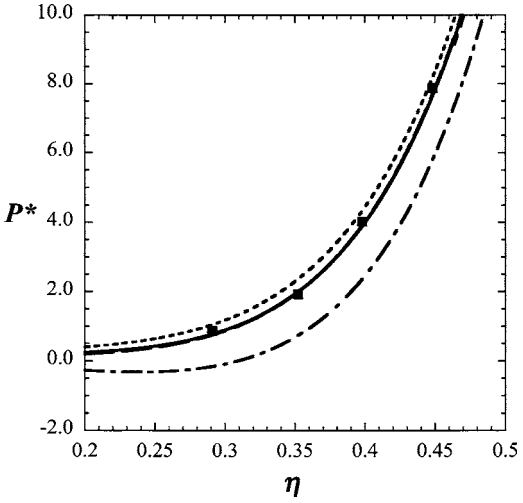


FIG. 4. Comparison of *NPT* MC simulation data for a symmetric electrolyte solution (system 2) at $T^*=1.8$ with $\varepsilon^*=1.0$, $\lambda=1.5$, $\sigma^{+*}=\sigma^{-*}=\sigma_d^*=1.0$, $\psi^*=5.0$, $r_c^*=1.05$, charge $q=1$, ion concentration of 8/256, and dipole moment $\mu^{*2}=1.0$ with predictions from the SAFT-VR+DE approach (solid line) and the Debye-Hückel (dash-dot line), restricted primitive (dotted line), primitive (short dashed line, hidden by the dotted line), restricted nonprimitive (long dashed line, hidden by the solid line), and seminonprimitive (medium dashed line, hidden by the solid line) models.

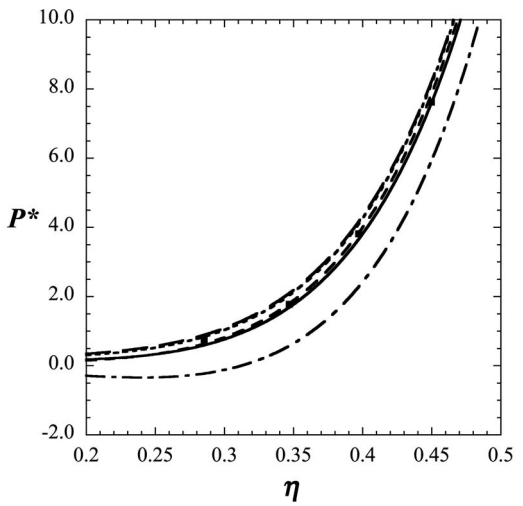


FIG. 6. Comparison of *NPT* MC simulation data for a semisymmetric model electrolyte solution (system 5) at $T^*=1.8$ with $\varepsilon^*=1.0$, $\lambda=1.5$, $\sigma_d^*=1.0$, $\sigma^{+*}=\sigma^{-*}=0.5$, $\psi^*=5.0$, $r_c^*=1.05$, charge $q=1$, ion concentration of 8/256, and dipole moment $\mu^{*2}=1.0$ with predictions from the SAFT-VR+DE approach (solid line) and the Debye-Hückel (dash-dot line), restricted primitive (dotted line), primitive (short dashed line, hidden by the dotted line), restricted nonprimitive (long dashed line), and seminonprimitive (medium dashed line) models.

constant from the nonprimitive model. The prediction from the SAFT-VR+DE EOS is in excellent agreement with the simulation data for the system studied, illustrating the need for both an accurate value of the dielectric constant and an accurate representation of the size asymmetry between the solvent and ions.

Since real electrolyte solutions, such as aqueous solutions of NaCl, are typically composed of ions of different sizes, it is desirable to be able to model asymmetric electrolyte solutions that are composed of ions and solvent of different diameters. To test the ability of the SAFT-VR+DE equation in this respect we have studied the *PVT* behavior of an asymmetric electrolyte solution in which the solvent, cation, and anion diameters are in the ratio 3:1:2 (system 6). The results are presented in Fig. 7, where again we see that the SAFT-VR+DE approach provides good agreement with the simulation data. From a comparison of systems 2, 5, and 6 [Figs. 2(b), 5, and 7] we note that the asymmetric system exhibits the highest density at given pressure and temperature, while the symmetric system has the lowest density. In Fig. 8, we again compare the theoretical predictions obtained from the SAFT-VR+DE equation with different models for incorporating the electrostatic interactions and *NPT* MC

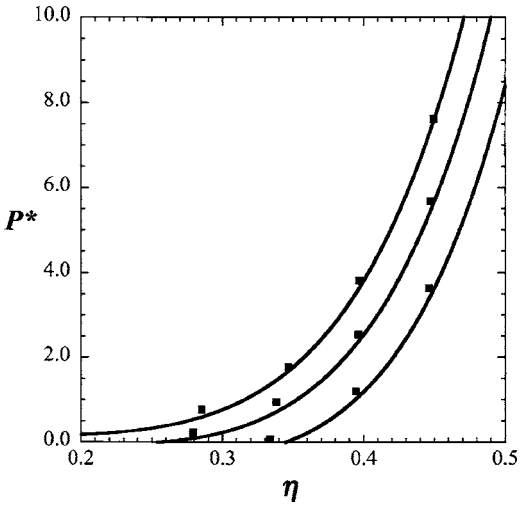


FIG. 5. Comparison of predictions from the SAFT-VR+DE approach and *NPT* MC simulation data for a semiasymmetric model electrolyte solution (system 5) with $\varepsilon^*=1.0$, $\lambda=1.5$, $\sigma_d^*=1.0$, $\sigma^{+*}=\sigma^{-*}=0.5$, $\psi^*=5.0$, $r_c^*=1.05$, charge $q=1$, ion concentration of 8/256, and dipole moment $\mu^{*2}=1.0$ at $T^*=1.4$, 1.6, and 1.8 (from bottom to top). The solid lines represent predictions from the SAFT-VR+DE equation and the squares the *NPT* MC simulation data.

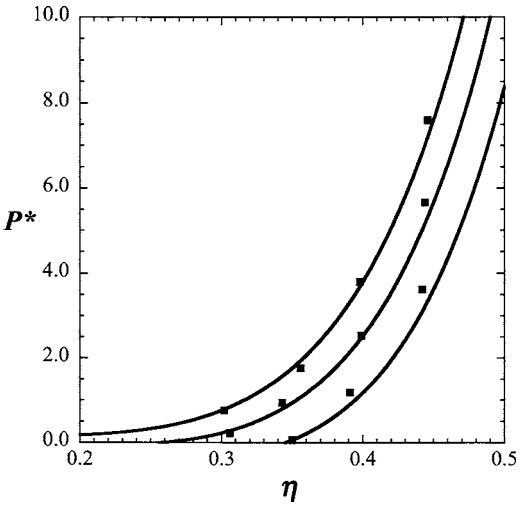


FIG. 7. Comparison of predictions from the SAFT-VR+DE approach and *NPT* MC simulation data for an asymmetric model electrolyte solution (system 6) with $\varepsilon^*=1.0$, $\lambda=1.5$, $\sigma_d^*=1.0$, $\sigma^{+*}=1/3$, $\sigma^{-*}=2/3$, $\psi^*=5.0$, $r_c^*=1.05$, charge $q=1$, ion concentration of 8/256, and dipole moment $\mu^{*2}=1.0$ at $T^*=1.4$, 1.6, and 1.8 (from bottom to top). The solid lines represent predictions from the SAFT-VR+DE equation and the squares the *NPT* MC simulation data.

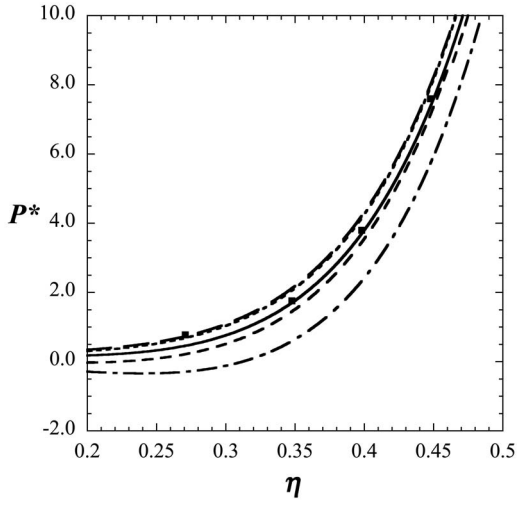


FIG. 8. Comparison of *NPT* MC simulation data for an asymmetric model electrolyte solution (system 6) at $T^*=1.8$ with $\varepsilon^*=1.0$, $\lambda=1.5$, $\sigma_d^*=1.0$, $\sigma^{+*}=1/3$, $\sigma^{-*}=2/3$, $\psi^*=5.0$, $r_c^*=1.05$, charge $q=1$, ion concentration of 8/256, and dipole moment $\mu^{*2}=1.0$ with predictions from the SAFT-VR +DE approach (solid line) and the Debye-Hückel (dash-dot line), restricted primitive (dotted line), primitive (short dashed line, hidden by the dotted line), restricted nonprimitive (long dashed line), and seminonprimitive (medium dashed line) models.

simulation data. From the figure for system 6 at $T^*=1.8$ we note similar trends to those observed for the semiasymmetric system studied: namely, the prediction from the SAFT-VR +DE EOS is in excellent agreement with the simulation data, while the predictions from the Debye-Hückel model exhibit the poorest agreement with the *NPT* MC simulation data, indicating that the effect of the size of the ions and solvent plays an important role in determining the thermodynamic properties of electrolyte solutions. We again note that the overall good agreement with the simulation data for the primitive models, which require the dielectric constant to be predetermined, is due to the use of the dielectric constant from the nonprimitive model. We also note from the comparison that the predictions using the seminonprimitive model, in which the effective size of ions is used, only slightly overpredicts the density at given pressure and temperature in comparison with the simulation data and SAFT-VR+DE approach.

## V. CONCLUSION

In this work, the SAFT-VR+DE approach has been developed through a combination of the SAFT-VR equation and the MSA solution for the nonprimitive model, in which the solvent molecules are explicitly described. The theoretical expressions needed to study the ion-ion, ion-dipole, and dipole-dipole interactions have been presented. *NPT* MC simulations were performed to obtain simulation data with which to compare the theoretical predictions and test the new approach. We find that the SAFT-VR+DE equation provides a good description of the *PVT* behavior of the electrolyte systems studied. We have also compared the SAFT-VR +DE equation with five other models for incorporating electrostatic interactions, namely, the Debye-Hückel theory, the primitive model (RPM and PM), the restricted nonprimitive model, and the semirestricted nonprimitive model. We find that the Debye-Hückel model shows the largest deviations from the Monte Carlo simulation data, indicating the importance of properly accounting for the difference in size between the ions and solvent if the thermodynamics of real electrolyte solutions are to be accurately described. We have also shown the importance of an accurate description of the dielectric constant and how the predictive capability of the primitive model and the Debye-Hückel theory strongly depends on the value of the dielectric constant. By using the nonprimitive model in the SAFT-VR+DE approach we avoid the need to provide input values for the dielectric constant, either by finding experimental data or developing correlations for mixed solvent electrolyte systems, and so expand the flexibility of the theory considerably over other SAFT based approaches for electrolyte solutions. We also find that the predictions obtained from the semirestricted nonprimitive model are very similar to those from the SAFT-VR+DE approach (i.e., nonprimitive model), indicating that an assumption of equal sized ions is reasonable. Given the relative simplicity of the semirestricted nonprimitive model, it may be advantageous to use this approximation when developing engineering equations of state for electrolyte solutions. Although we have only tested the proposed SAFT-VR+DE approach for relatively dilute electrolyte solutions and monomer ions and solvent, our approach is generally applicable and can easily be applied to more concentrated electrolyte solutions and chainlike ions and/or solvent through the addition of a chain term in which the pair distribution function can be derived from the mean spherical approximation.[44]

## ACKNOWLEDGMENT

The authors gratefully acknowledge financial support from the National Science Foundation under Grant No. CTS-0452688.

## APPENDIX: DEFINITION OF MODELS

### 1. Debye-Hückel

The Helmholtz free energy is given by

$$\frac{A^{\mathrm{DH}}}{NKT}=-\frac{\kappa^3}{12\pi\rho}, \tag{A1}$$

where $\kappa$ is the inverse Debye screening length,

$$\kappa^2=\frac{4\pi z^2 e^2 \rho\beta}{\varepsilon}. \tag{A2}$$

### 2. RPM of the MSA

The Helmholtz free energy is given by

$$\frac{A^{\mathrm{RPM}}}{NKT}=-\frac{3x^2+6x+2-2(1+2x)^{3/2}}{12\pi\rho\sigma^3}, \tag{A3}$$

with $x=\kappa\sigma$.

### 3. The primitive model of the MSA

The Helmholtz free energy can be expressed by

$$\frac{A^{\mathrm{PM}}}{NKT} = -\frac{1}{\rho}\left[\frac{\beta e^2}{4\pi\varepsilon}\sum_k \frac{\rho_k z_k}{1+\Gamma\sigma_k}\left(\Gamma z_k + \frac{\pi P_n \sigma_k}{2\Delta}\right) - \frac{\Gamma^3}{3\pi}\right], \tag{A4}$$

where $\Delta = 1-\xi_3$ and $\Gamma$ is the scaling parameter that can be calculated from

$$\Gamma^2 = \frac{\beta e^2}{4\varepsilon}\sum_k \frac{\rho_k z_k}{(1+\Gamma\sigma_k)^2}\left(z_k - \frac{\pi P_n \sigma_n^2}{2\Delta}\right)^2, \tag{A5}$$

with

$$P_n = \frac{\sum_k \rho_k \sigma_k z_k/(1+\Gamma\sigma_k)}{1+(\pi/2\Delta)\sum_k \rho_k \sigma_k^3/(1+\Gamma\sigma_k)}. \tag{A6}$$

### 4. Seminonprimitive model of the MSA

The electrolyte solution is modeled as a mixture of ions and dipoles. The ions are hard spheres of diameter of $\sigma_i$, half with charge $+q$ and half with charge $-q$. The dipoles are hard spheres of diameter $\sigma_d$, with a central point dipole of magnitude $\mu$. The ratio between the diameter of dipolar hard spheres and the diameter of ions is defined by

$$p = \sigma_d/\sigma_i. \tag{A7}$$

The solution is given in terms of two independent variables, which represent the reduced values of the ionic charge and the dipoles, respectively,

$$d_0^2 = \frac{4\pi q^2 \rho_i \sigma_i^2}{kT}, \qquad d_2^2 = \frac{4\pi\mu^2\rho_d}{3kT} = y. \tag{A8}$$

The solution of the MSA is given in terms of the three energy parameters, $b_0$ (ion-ion), $b_1$ (ion-dipole), and $b_2$ (dipole-dipole), and the three parameters satisfy the following set of equations:

$$a_1^2 + a_2^2 = d_0^2, \qquad a_1 K_{10} - a_2[1-K_{11}] = d_0 d_2, \qquad K_{10}^2 + [1-K_{11}]^2 - y_1^2 = d_2^2, \tag{A9}$$

where

$$a_1 = \frac{\Delta - 2\beta_6 D_F}{2D_F^2}, \qquad a_2 = \frac{-b_1}{2\beta_6 D_F^2}\left[\frac{\Delta}{2} + \frac{\beta_3 D_F}{p}\right], \qquad K_{10} = p\frac{b_1}{2\Delta}[1+a_1\Lambda],$$

$$1-K_{11} = \frac{\beta_3 - (p/2)a_2 b_1 \Lambda}{\Delta}, \qquad y_1 = \frac{\beta_6}{\beta_{12}^2}, \qquad D_F = \frac{1}{2}\left[\beta_6(1+b_0) - \frac{b_1 p}{12}\right],$$

$$\Delta = b_1^2/4 + \beta_6^2, \qquad \Lambda = \frac{1+b_0}{2} + \frac{p}{6}\beta_6, \qquad \beta_3 = 1 + b_2/3, \qquad \beta_6 = 1 - b_2/6,$$

$$\beta_{12} = 1 + b_2/12, \qquad \beta_{24} = 1 - b_2/24. \tag{A10}$$

The excess Helmholtz free energy is given by

$$\frac{A^{\mathrm{MSA}}}{NKT} = \frac{1}{12\pi\rho\sigma_d^3}[2p^3 d_0^2 b_0 - 2p^2 d_0 d_2 b_1 - J'], \qquad J' = p^3 Q_{ii}^2 + p(p+1)Q_{id}^2 + Q_{dd}^2 + 2q'^2, \tag{A11}$$

where

$$Q_{ii} = -a_1 + 2 + \frac{\beta_6}{D_F}, \qquad Q_{id} = \frac{b_1}{\Delta}[\beta_3 + a_1(3\Lambda - 2D_F)], \qquad Q_{dd} = \frac{1}{\Delta}[2\beta_3^2 - p b_1 a_2(3\Lambda - 2D_F)] - 2, \qquad q' = b_2\beta_{24}/\beta_{12}^2. \tag{A12}$$

The excess chemical potentials for ions and dipoles are expressed as

$$\frac{\mu_i^{\mathrm{MSA}}}{KT} = (q^*)^2\left(b_0 - \frac{d_2 b_1}{d_0 p}\right), \qquad \frac{\mu_d^{\mathrm{MSA}}}{KT} = -\frac{(\mu^*)^2}{3}\left(2b_2 + \frac{d_0 b_1 p^2}{d_2}\right), \tag{A13}$$

where

$$q^* = q/k_B T\sigma_i.$$

The excess internal energy of the system is given by

$$\frac{U^{\mathrm{MSA}}}{NKT} = \frac{1}{4\pi\rho\sigma_d^3}[p^3 d_0^2 b_0 - 2p^2 d_0 d_2 b_1 - 2d_2^2 b_2]. \quad \text{(A14)}$$

In the MSA, the excess Gibbs free energy equals the excess internal energy. Thus, the compressibility factor can be given as

$$Z^{\mathrm{MSA}} = \frac{P^{\mathrm{MSA}}}{\rho KT} = \frac{U^{\mathrm{MSA}} - A^{\mathrm{MSA}}}{NKT}. \quad \text{(A15)}$$


[1] J. V. Sengers, R. F. Kayser, C. J. Peters, and H. J. White, *Equations of State for Fluids and Fluid Mixtures* (Elsevier, Amsterdam, 2000).
[2] K. S. Pitzer, J. Phys. Chem. **77**, 268 (1973).
[3] C. C. Chen, H. I. Britt, J. F. Boston, and L. B. Evans, AIChE J. **28**, 588 (1982); C. C. Chen and L. B. Evans, *ibid.* **32**, 444 (1986).
[4] G. Stell and J. L. Lebowitz, J. Chem. Phys. **49**, 3706 (1968).
[5] D. Henderson, ACS Symp. Ser. **204**, 47 (1983).
[6] H. L. Friedman, Annu. Rev. Phys. Chem. **32**, 179 (1981).
[7] P. T. Cummings and G. Stell, Mol. Phys. **44**, 529 (1981).
[8] D. Henderson, L. Blum, and A. Tani, ACS Symp. Ser. **300**, 281 (1986).
[9] K. Y. Chan, J. Phys. Chem. **95**, 7465 (1991).
[10] G. Jin and M. D. Donohue, Ind. Eng. Chem. Res. **27**, 1073 (1988); **27**, 1737 (1988); **30**, 240 (1991).
[11] P. Vimalchand, I. Celmins, and M. D. Donohue, AIChE J. **32**, 1735 (1986).
[12] Y. Rosenfeld and L. Blum, J. Phys. Chem. **89**, 5149 (1985); J. Chem. Phys. **85**, 1556 (1986).
[13] D. Chandler and H. C. Andersen, J. Chem. Phys. **57**, 1930 (1972).
[14] F. Hirata and P. J. Rossky, Chem. Phys. Lett. **83**, 329 (1981); F. Hirata, P. J. Rossky, and B. M. Pettitt, J. Chem. Phys. **78**, 4133 (1983).
[15] J. A. Barker and D. Henderson, Rev. Mod. Phys. **48**, 587 (1976).
[16] E. Waisman and J. L. Lebowitz, J. Chem. Phys. **56**, 3086 (1972); **56**, 3093 (1972).
[17] L. Blum, Mol. Phys. **30**, 1529 (1975).
[18] L. L. Lee, *Molecular Thermodynamics of Nonideal Fluids* (Butterworth-Heinemann, Boston, 1988).
[19] F. X. Ball, H. Planche, W. Furst, and H. Renon, AIChE J. **31**, 1233 (1985).
[20] J. F. Lu, Y. X. Yu, and Y. G. Li, Fluid Phase Equilib. **85**, 81 (1993).
[21] L. Blum, J. Chem. Phys. **61**, 2129 (1974); L. Blum and J. S. Hoye, J. Phys. Chem. **81**, 1311 (1977).
[22] S. A. Adelman and J. M. Deutch, J. Chem. Phys. **60**, 3935 (1974).
[23] L. Blum and D. Q. Wei, J. Chem. Phys. **87**, 555 (1987).
[24] J. S. Hoye and G. Stell, J. Chem. Phys. **68**, 4145 (1978); **71**, 1985 (1979).
[25] C. X. Li, Y. G. Li, J. F. Lu, and L. Y. Yang, Fluid Phase Equilib. **124**, 99 (1996).
[26] J. R. Loehe and M. D. Donohue, AIChE J. **43**, 180 (1997).
[27] A. Anderko, P. M. Wang, and M. Rafal, Fluid Phase Equilib. **194**, 123 (2002).
[28] W. G. Chapman, K. E. Gubbins, G. Jackson, and M. Radosz, Fluid Phase Equilib. **52**, 31 (1989); Ind. Eng. Chem. Res. **29**, 1709 (1990).
[29] M. S. Wertheim, J. Stat. Phys. **35**, 19 (1984); **35**, 35 (1984); **42**, 459 (1986); **42**, 477 (1986).
[30] E. A. Muller and K. E. Gubbins, Ind. Eng. Chem. Res. **40**, 2193 (2001).
[31] I. G. Economou, Ind. Eng. Chem. Res. **41**, 953 (2002).
[32] A. Gil-Villegas, A. Galindo, P. J. Whitehead, S. J. Mills, G. Jackson, and A. N. Burgess, J. Chem. Phys. **106**, 4168 (1997).
[33] A. Galindo, L. A. Davies, A. Gil-Villegas, and G. Jackson, Mol. Phys. **93**, 241 (1998).
[34] C. McCabe and G. Jackson, Phys. Chem. Chem. Phys. **1**, 2057 (1999); C. McCabe, A. Galindo, M. N. Garcia-Lisbona, and G. Jackson, Ind. Eng. Chem. Res. **40**, 3835 (2001); C. McCabe and S. B. Kiselev, Fluid Phase Equilib. **219**, 3 (2004); Ind. Eng. Chem. Res. **43**, 2839 (2004).
[35] C. McCabe, A. Galindo, A. Gil-Villegas, and G. Jackson, Int. J. Thermophys. **19**, 1511 (1998).
[36] C. McCabe, A. Gil-Villegas, and G. Jackson, J. Phys. Chem. B **102**, 4183 (1998); A. Galindo, L. J. Florusse, and C. J. Peters, Fluid Phase Equilib. **160**, 123 (1999); E. J. M. Filipe, E. de Azevedo, L. F. G. Martins, V. A. M. Soares, J. C. G. Calado, C. McCabe, and G. Jackson, J. Phys. Chem. B **104**, 1315 (2000); E. J. M. Filipe, L. F. G. Martins, J. C. G. Calado, C. McCabe, and G. Jackson, *ibid.* **104**, 1322 (2000); E. J. M. Filipe, L. M. B. Dias, J. C. G. Calado, C. McCabe, and G. Jackson, Phys. Chem. Chem. Phys. **4**, 1618 (2002); L. M. B. Dias, E. J. M. Filipe, C. McCabe, and J. C. G. Calado, J. Phys. Chem. B **108**, 7377 (2004); L. X. Sun, H. G. Zhao, S. B. Kiselev, and C. McCabe, *ibid.* **109**, 9047 (2005); L. Sun, H. Zhao, and C. McCabe, AIChE J. **53**, 720 (2007); H. G. Zhao, P. Morgado, C. McCabe, and A. Gil-Villegas, J. Phys. Chem. B **110**, 24083 (2006).
[37] L. X. Sun, H. G. Zhao, S. B. Kiselev, and C. McCabe, Fluid Phase Equilib. **228**, 275 (2005).
[38] C. McCabe, A. Galindo, A. Gil-Villegas, and G. Jackson, J. Phys. Chem. B **102**, 8060 (1998); R. P. Bonifacio, E. J. M. Filipe, C. McCabe, M. F. C. Gomes, and A. A. H. Padua, Mol. Phys. **100**, 2547 (2002); P. Morgado, C. McCabe, and E. J. M. Filipe, Fluid Phase Equilib. **228**, 389 (2005); P. Morgado, H. Zhao, F. J. Blas, C. McCabe, L. P. N. Rebelo, and E. J. M. Filipe, J. Phys. Chem. B **111**, 2856 (2005).
[39] A. Galindo, S. J. Burton, G. Jackson, D. P. Visco, and D. A. Kofke, Mol. Phys. **100**, 2241 (2002);
[40] L. M. B. Dias, R. P. Bonifacio, E. J. M. Filipe, J. C. G. Calado, C. McCabe, and G. Jackson, Fluid Phase Equilib. **205**, 163 (2003).
[41] C. McCabe, A. Galindo, and P. T. Cummings, J. Phys. Chem. B **107**, 12307 (2003); A. Valtz, A. Chapoy, C. Coquelet, P. Paricaud, and D. Richon, Fluid Phase Equilib. **226**, 333 (2004).
[42] A. Galindo, A. Gil-Villegas, P. J. Whitehead, G. Jackson, and A. N. Burgess, J. Phys. Chem. B **102**, 7632 (1998).
[43] F. J. Blas and A. Galindo, Fluid Phase Equilib. **194–197**, 501 (2002); A. Galindo and F. J. Blas, J. Phys. Chem. B **106**, 4503 (2002); C. M. Colina, A. Galindo, F. J. Blas, and K. E. Gubbins, Fluid Phase Equilib. **222**, 77 (2004); C. M. Colina and K. E. Gubbins, J. Phys. Chem. B **109**, 2899 (2005).
[44] H. Zhao and C. McCabe, J. Chem. Phys. **125**, 4504 (2006).
[45] W. B. Liu, Y. G. Li, and J. F. Lu, Fluid Phase Equilib. **160**, 595 (1999).
[46] J. Z. Wu and J. M. Prausnitz, Ind. Eng. Chem. Res. **37**, 1634 (1998).
[47] S. P. Tan, H. Adidharma, and M. Radosz, Ind. Eng. Chem. Res. **44**, 4442 (2005).
[48] L. F. Cameretti, G. Sadowski, and J. M. Mollerup, Ind. Eng. Chem. Res. **44**, 3355 (2005).
[49] A. Galindo, A. Gil-Villegas, G. Jackson, and A. N. Burgess, J. Phys. Chem. B **103**, 10272 (1999).
[50] A. Gil-Villegas, A. Galindo, and G. Jackson, Mol. Phys. **99**, 531 (2001).
[51] B. H. Patel, P. Paricaud, A. Galindo, and G. C. Maitland, Ind. Eng. Chem. Res. **42**, 3809 (2003).
[52] P. J. Leonard, D. Henderson, and J. A. Barker, Trans. Faraday Soc. **66**, 2439 (1970).
[53] T. Boublik, J. Chem. Phys. **53**, 471 (1970).
[54] G. A. Mansoori, N. F. Carnahan, K. E. Starling, and T. W. Leland, J. Chem. Phys. **54**, 1523 (1971).
[55] D. Q. Wei and L. Blum, J. Chem. Phys. **87**, 2999 (1987).
[56] S. A. Adelman, J. Chem. Phys. **64**, 724 (1976).
[57] W. G. Chapman, G. Jackson, and K. E. Gubbins, Mol. Phys. **65**, 1057 (1988).
[58] G. Jackson, W. G. Chapman, and K. E. Gubbins, Mol. Phys. **65**, 1 (1988).
[59] J. A. Barker and R. O. Watts, Mol. Phys. **26**, 789 (1973); J. A. Barker, *ibid.* **83**, 1057 (1994).
[60] D. P. Visco and D. A. Kofke, J. Chem. Phys. **110**, 5493 (1999).
[61] H. G. Zhao, Y. Y. Ding, and C. McCabe, J. Phys. Chem. B (submitted).